EXPERIMENTAL STUDY OF DYNAMICS DURING CRUSHING OF FRESHWATER TRUNCATED CONICAL ICE SPECIMENS

Kashfi B. Habib
Centre for Arctic Resource Development, C-CORE
St. John's, NL, Canada

Rocky S. Taylor[1, 2]
[1]Memorial University of Newfoundland,
St. John's, NL, Canada
[2]Centre for Arctic Resource Development, C-CORE
St. John's, NL, Canada

Stephen Bruneau
Memorial University of Newfoundland,
St. John's, NL, Canada

Ian J. Jordaan
Memorial University of Newfoundland,
St. John's, NL, Canada

ABSTRACT

Ice crushing dynamics in ice structure interactions can result in hazardous vibrations and potentially damaging loads on offshore structures. Ice cone crushing experiments were conducted in the lab to characterize loading and dynamics processes for compressive failure. The indentation rate, temperature and shape of the ice specimens were varied in control tests so that the sensitivity of the resultant dynamic ice load frequency and amplitude could be determined. The results indicate that all control variables had a marked effect on both the frequency and amplitude of load fluctuations. Indentation rates varying from 0.1 mm/s to 10 mm/s and ice taper angles from 13° to 30° had drastic effects. The effects of temperature also demonstrated variations in force, pressure and dynamic behavior. In addition to load measurements, video was used to observe failure mechanisms and in particular spalling and crushing. In the present paper observations are described, though a thorough quantitative assessment has been published elsewhere. Tactile pressure sensors were also used in the experiments, allowing for the correlation of loads and processes to pressure distributions. Finally, the forensic examination of crushed specimens also provided insights into the behavior of ice under various compressive failure scenarios. On the surfaces of intact specimens and revealed within through cross-polarized views of thin sections were signs of ice damage and recrystallization zones of varying extents. The effects of the variables on the dynamic processes and failure behaviors are discussed.

INTRODUCTION

Dynamic response and associated ice induced vibrations pose a significant design challenge for offshore structures, drilling platforms, and bridge piers in sea ice environments. The compressive failure of ice can cause severe dynamic load on these structures. Extreme resonant vibrations can cause extensive damage to the facilities, which can lead to fatigue failure in either structural or non-structural elements. Ice failure dynamic is a complex process and the development of models of these phenomena is not straightforward. Dynamic response varies with the applied loading rate, as well as the temperature, ice type and shape of the ice and other loading conditions. For full-scale interactions this is complicated by the fact that the ice may experience different failure modes during an interaction such as bending, crushing, spalling and splitting fracture.

To understand the characteristics of dynamics under ice structure interaction, many researchers have been working since the 1970s by applying different approaches to model ice induced vibrations ([1]-[9]). More recent works on dynamic ice forces have been carried out by a number of researchers as can be seen in [10]-[16].

Dynamic processes can be categorized into different categories. Matlock et al. [17] classified the model as a series of discrete or intermittent events occurring at low ice velocity. Sodhi [18] extended this model to overcome the limitations by introducing loading and extrusion phases. Blenkarn [2] and Määttänen [19] modeled ice failure as a continuous crushing process. In this approach, non-simultaneous ice crushing is modeled during high ice velocity at the contact interface but at low velocity a ductile to brittle transition is produced with a simultaneous ice failure process. Huang and Liu [14] modified the Matlock-Sodhi model to account for the velocity effect and to include stochastic characteristics of ice crushing. To describe dynamic behavior, Palmer et al. [15] classified different structure displacement responses in time into the four categories outlined in Figure 1 based on ISO 19906 [20], Yue et al. [21], Bjerkås [22], Bjerkås and Skiple [23], Jefferies and Wright [24] and Sodhi [13].
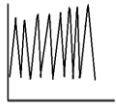
Mode	1	2	3	4
Structure displacement schematic response				
Nomenclature				
Palmer et al. [15]	Creep	Quasi-static	Locked-in	Random
Draft ISO 19906 [20]		Intermittent	Frequency lock-in	Continuous brittle
Yue et al. [21]		Quasi-static	Locked-in	Random
Bjerkas [22]		Quasi-static	Steady state crushing	Random
Jefferies and Wright [24]		Sawtooth	Phase-locked	
Sodhi [13]	Creep	Intermittent crushing	Intermittent crushing	Continuous crushing

Figure 1: Dynamics mode defined after Palmer et al. [15]

A series of small-scale indentation tests have been conducted for this program to study the influence of different test variables on ice failure processes and associated dynamic behavior. This work aims to understand the responses and characteristics of ice crushing dynamics under different loading conditions (crushing rate, temperature and ice shape). Particular attention was paid to the frequencies and amplitudes of the force during ice crushing. During small-scale tests, the most common load limiting factors are spalling and crushing ([25] - [30]). Spalling is referred to as localized fracture that leads to a loss of significant contact area from the ice-structure interface. Spalling is a very irregular process that initiates from cracks near the high pressure zones and is promoted by the flaws

present in the ice [12]. On the other hand, crushing is defined as the pulverization and extrusion of softened ice from the periphery of the high pressure zones. Crushing has been observed to produce cyclic loadings and is associated with the formation and failure of high pressure zones ([25]-[34]). By analyzing the regular and hi-speed videos, crushing is characterized as a continuous extrusion of fine grained material from the periphery of the indenter. To consistently identify periods of crushing failure, load cell data and video recordings of the experiments were examined.

Prior experiments on ice indentation provide an important background for the research presented herein (see [26]-[29], [33]-[40]). In the present program, laboratory experiments were conducted as a cost-effective means to study the influence of indentation rate, temperature and ice shape on ice crushing dynamics processes during the indentation of truncated conical ice specimens. In the sections below, a summary of the experimental setup and results from recent laboratory experiments are provided. For additional details and all the results please see [33].

EXPERIMENTAL SETUP

Ice specimens were produced using freshwater, polycrystalline ice pieces that were crushed into ice seeds and sieved into two different size ranges: 0-4 mm and 4-10$^+$ mm. Distillation, deionization and deaeration processes were followed to prepare the water for the ice samples. The cooled water and ice seeds were compacted in a mold and placed into the freezer at -25°C. The bottom portion of the mold also served as a confining ring, which remained affixed to the ice during the crushing tests. Following two days of freezing, the samples were shaped to the desired profiles using an ice shaping apparatus. As illustrated in Figure 2, the conical truncated ice specimens were used with an average diameter of 268.8 mm at the bottom and 25.4 mm at the top. Ice specimens with three different taper angles were considered: 13°, 21° and 30°. After the shaping, the specimens were covered and stored in a cold room for at least twenty-four (24) hours to adjust to the target temperature [41]. A detailed description of the experimental setup is given in [33] and [38].

For this test program, the Materials Testing System (MTS) at Memorial University of Newfoundland was used for experimentation and the load cell data as shown in Figure 3(a). Before the experiments, an indenter plate was mounted to the primary load cell, which was fixed to the MTS cross-head. For testing, the prepared ice specimens were mounted on the MTS base plate attached to the hydraulic ram. The hydraulic ram was used to control vertical displacement and the indentation rate of the mounted specimen, while the indenter plate and the MTS crosshead remained fixed. Two different shaped indenters were used in the experiments. A flat indenter with a diameter of 256 mm and a thickness of 19 mm was used in most of the experiments. The spherical indenter had the same diameter as

the flat indenter (256 mm) but the radius of the curvature was 325.12 mm.
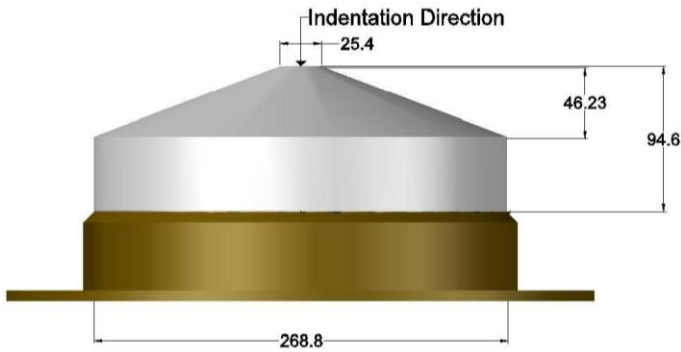

Figure 2: Geometry of an ice specimen having a taper angle of 21° (all dimensions are in mm)

To provide additional insights into the nature and variation of contact pressures, a tactile pressure sensor was placed at the ice-indenter interface. The sensor provides a pressure distribution recording which was correlated to the load cell data and failure processes. The handle of the sensor was mounted on the MTS machine with clamps to keep the sensor straight and fixed along the indenter plate as the ice specimen moved upward. The indentation for each test was done from the top surface of the ice sample to a depth of 70 mm. The data collected from the MTS load cell was the force against indentation depth and time. Regular and hi-speed video recordings were also carried out to capture the crushing behaviors and failure mechanisms during the indentation tests. Thin-sections of the damaged and parent ice were also prepared using the double-microtome technique developed by Sinha [42] to study the internal structures and grain size distributions of ice. These thin sections have also helped to provide insight into the characteristics of the damaged layer and associated processes. In Figure 3(b), images of the setup of an ice sample before and after the experiment are shown. The test matrix for the program is given in Table 1.

To calculate the frequency and amplitude of the dynamics of the ice tests, the load cell data were observed to determine continuous crushing events. The video recordings and tactile pressure distribution recordings were also compared with the load cell data for that time period to confirm crushing failure. It should be noted that determining the frequency and amplitude is not straightforward for a test as it can vary with displacement and also irregular spalling events during the experiment can largely influence the crushing events. For this reason, periods of dynamic activity, which are simply referred to as dynamic 'events', during each test were identified for the purposes of these analyses.
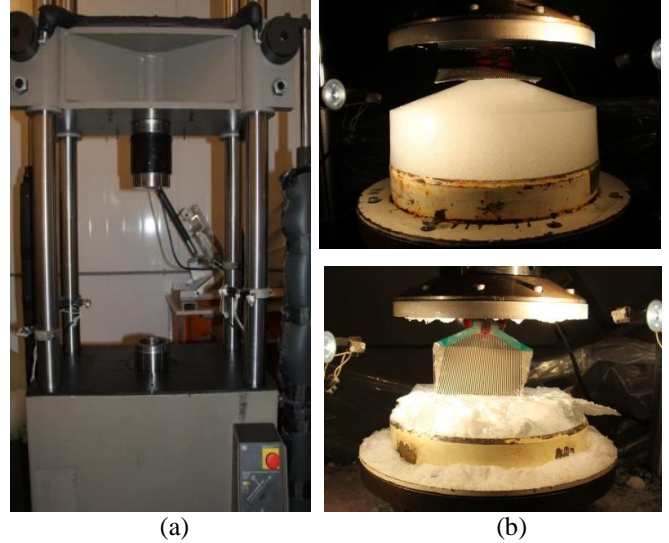

(a)   (b)

Figure 3: (a) MTS load frame (b) Arrangements of the indenter, ice sample and Tekscan sensor with MTS load frame before (top) and after (bottom) the test

Table 1: Test Matrix

Test No	Ind. Rate (mm/s)	Taper Angle (°)	Grain Size (mm)	Temperature (°C)	Indenter
1	0.1	21	4-10$^+$	-10	Flat
2	0.1	21	0-4	-10	Flat
3	1	21	4-10$^+$	-10	Flat
4	10	21	4-10$^+$	-10	Flat
5	1	21	0-4	-10	Flat
6	10	21	0-4	-10	Flat
7	10	21	0-4	-10	Spherical
8	10	21	4-10$^+$	-10	Spherical
9	10	30	4-10$^+$	-10	Spherical
10	10	30	0-4	-10	Spherical
11	0.1	30	4-10$^+$	-10	Flat
12	10	30	0-4	-10	Flat
13	1	30	4-10$^+$	-10	Flat
14	1	30	0-4	-10	Flat
15	10	30	4-10$^+$	-10	Flat
16	0.1	30	0-4	-10	Flat
17	0.1	13	4-10$^+$	-10	Flat
18	0.1	13	0-4	-10	Flat
19	1	13	4-10$^+$	-10	Flat
20	1	13	0-4	-10	Flat
21	10	13	4-10$^+$	-10	Flat
22	10	13	0-4	-10	Flat
23	10	13	4-10$^+$	-10	Spherical
24	1	13	4-10$^+$	-10	Spherical
25	0.1	21	4-10$^+$	-5	Flat
26	1	21	4-10$^+$	-5	Flat
27	10	21	4-10$^+$	-5	Flat
28	10	21	0-4	-5	Flat

RESULTS AND DISCUSSION

A total of twenty-eight experiments were completed for this study using samples made with bigger grain size (4-10$^+$ mm) and smaller grain size ice seeds (0-4mm). These experiments were done at two different temperatures. Twenty-four tests were done at -10°C and four tests were done at -5°C.

Three crushing rates were applied for the indentation (slow test: 0.1 mm/s, medium test: 1 mm/s and fast test: 10 mm/s) using flat and curved indenters. The influence of the ice shape (samples with taper angle: 13°, 21°, 30°) has also been considered. In this paper the effects of crushing rate, temperature and taper angle on ice crushing dynamics are discussed in detail. The load cell data, pressure distribution results from tactile pressure sensors, recorded video observations and thin section images have been used to relate the cause of the dynamic behaviors.

Influence of Crushing Rate

Indentation rates have significant effects on crushing behaviors and dynamic processes. The slow tests (0.1 mm/s) exhibit continuous damage-enhanced creep behavior throughout the tests. The medium speed tests (1 mm/s) have a combination of crushing and fracture failure. The fast tests (10 mm/s) experience brittle failure and show many random fractures during the tests; see also [34].

In Figure 4(a) force-displacement plots are given for three tests with different crushing rates up to the indentation depth of 25 mm. These tests were done at -10°C with a flat indenter. During the slow test (0.1 mm/s) the sample experienced slow 'ductile' failure with a continuously increasing trend of load. During the medium speed test (1 mm/s) brittle failure with random crushing and spalling failure events occurred during the first few seconds, and as the force started to build up, the failure transitioned from a brittle to ductile mode with the gradually increasing load. In the fast speed test (10 mm/s) the first few seconds of the test showed a combination of 'ductile' and intermittent crushing failure, but as it proceeded, it exhibited continuous crushing failure. The loading effects on spalled ice particles, post-test geometry and damage state images are discussed in [34].

To observe the dynamic processes a closer look from Figure 4(a) is shown in Figure 4(b) and corresponding pressure distributions from the pressure sensor are given in Figure 4(c). Events 1-4 (slow test) showed a slight increase of load with a small increase of interaction area from 9 to 11 mm of indentation, without any significant increase of the pressure.

Medium speed test events showed examples of crushing failures in events 5 to 6 and 7 to 8. In these cases the contact areas increased but without any significant change in the shapes. A spalling failure occurred from event 6 to event 7 that was also observed from the pressure sensor image which showed a large, asymmetric area drop with a loss of some high pressure zones.

Fast test events (9-12) show examples of crushing that followed a same trend of failure for a period of time where no big spalls were spotted with only small area losses from the periphery of the contact pressure.
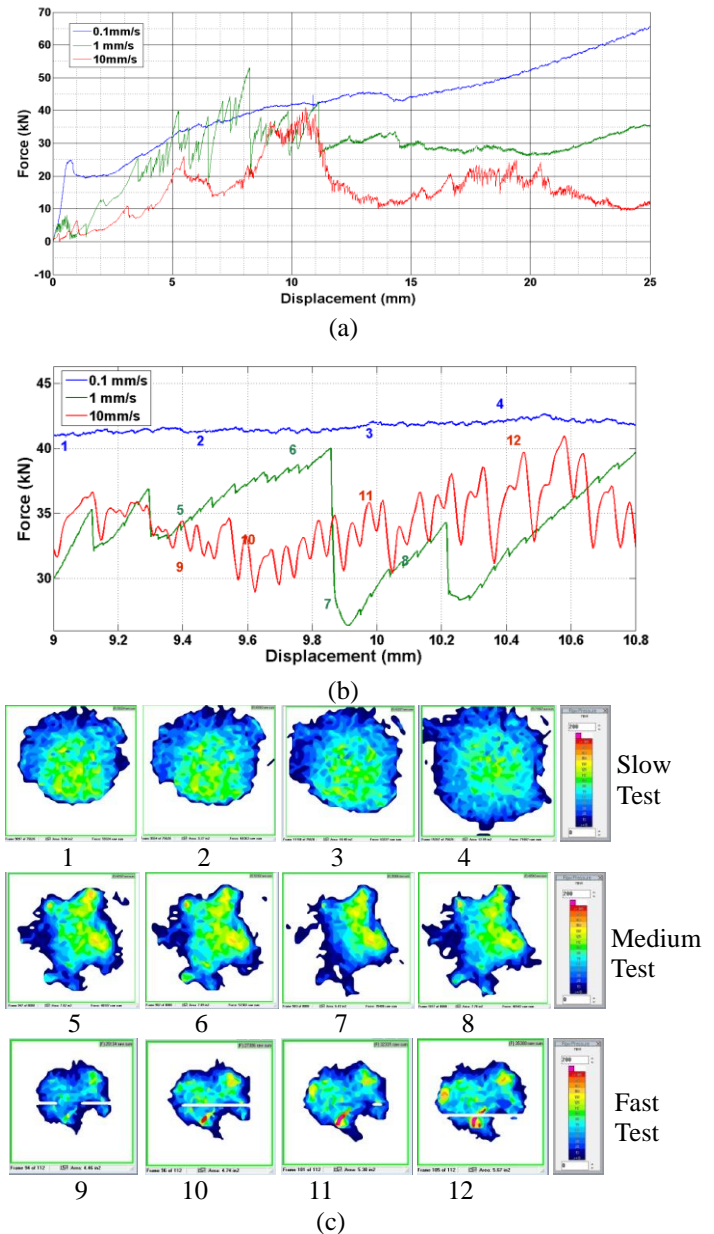

(a)

(b)

(c)

Figure 4: (a) MTS load cell data, (b) MTS load cell data from 9 to 11 mm displacement, (c) pressure sensor images for three different speed tests: Slow speed test (Test 17: blue); Medium speed test (Test 19: green); Fast speed test (Test 21: red)

The dynamics of the experiments change as the conditions of loading rates change. In Figure 5, the frequencies of cyclic loadings for three indentation rates are shown for three different cases. The frequencies were calculated from observed continuous crushing events for a certain period of time to exclude any possibility of random failure as spalling in that period. The slow speed tests did not show any cyclic behavior in any of the three cases, but in fast speed cases the frequencies increased about 5 to 10 times from the frequencies of medium speed cases. Browne [27] had used confined ice samples to do

similar small-scale ice crushing experiments. Using three different crushing rates in a medium speed range, similar results are found at -10°C (Figure 5). In addition it is noted that the nature of the cyclic response is significantly different for the ice at -5°C, as is explored further in the next section.
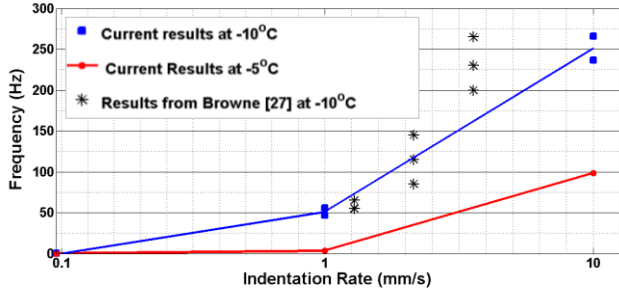

Figure 5: Frequency based on indentation rate

To relate the dynamic behaviors with the after crushing damage, the thin-section pictures (Figure 6) present details of the microstructural modifications at three different indentation speeds. Recrystallization effects are visible from the vertical thin sections that used cross polarized lights (color) and microfractures are clearly seen from the horizontal thin sections using a side lighting technique (black and white). The thin-sections in Figure 6(a) for the slow test show that the sample is heavily dominated by microfracture and recrystallization with the depth of the damaged area about 35 mm from the end point of the test. In the case of the medium speed test in Figure 6(b), both recrystallization and microfracture have an effect to a depth of about 15-20 mm in vertical image. The fast test in Figure 6(c) shows recrystallization is concentrated in the immediate crushing zone, and only extends to a depth of about 10 mm. The test also has less microfracture than other cases, suggesting that the damage was much more localized; tests at this speed also were characterized by more random spalls than tests at slower speeds ([34]).

(a) 0.1 mm/s   (b) 1 mm/s   (c) 10mm/s
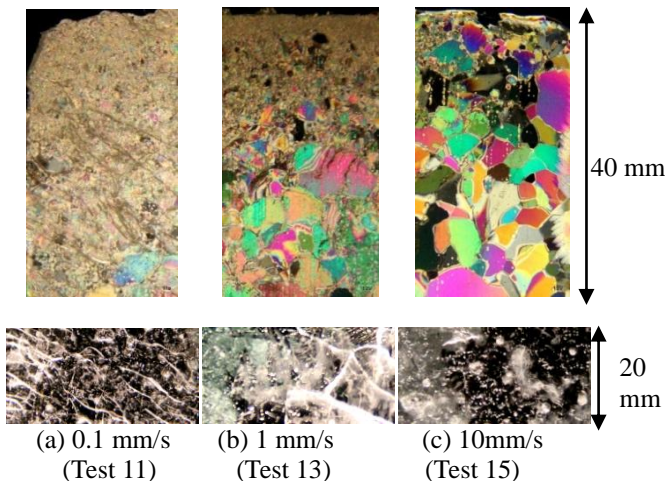(Test 11)   (Test 13)   (Test 15)

Figure 6: Vertical thin-section images using cross polarized light (color, top) and horizontal thin-section images using side lighting technique (black and white, bottom)

Influence of Ice Temperature

By investigating different cases, it was observed that the warmer test exhibits more ductile failure with higher loads, dominated by damage, while the cold test experienced more brittle failure [34]. The failure effect of temperature on the load cell data can be seen in Figure 7(a). In Figure 7(b), a clear image of dynamics can be seen from 4 to 5 mm of indentation. It should be noted that the large load drops also occurred in the warm tests due to spalling events, but there were fewer cyclic loadings in those cases.

To investigate the influence of temperature on dynamics, all the warm tests were observed individually. The results show that the warm tests (-5°C) experienced damage-enhanced creep and slow continuous crushing failure, while the colder tests (-10°C) showed mostly crushing failure when all the other parameters were held constant. The major load drops in the warm test (Figure 7(a)) at 5.4 mm and 9.7 mm were mainly due to the spalling events, which were also confirmed from the recorded videos. While observing the crushing failure, frequencies in the warm tests were much less than the cold tests as represented in Figure 5.
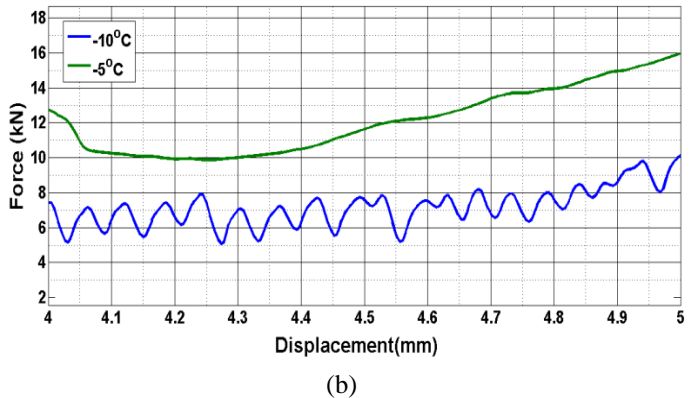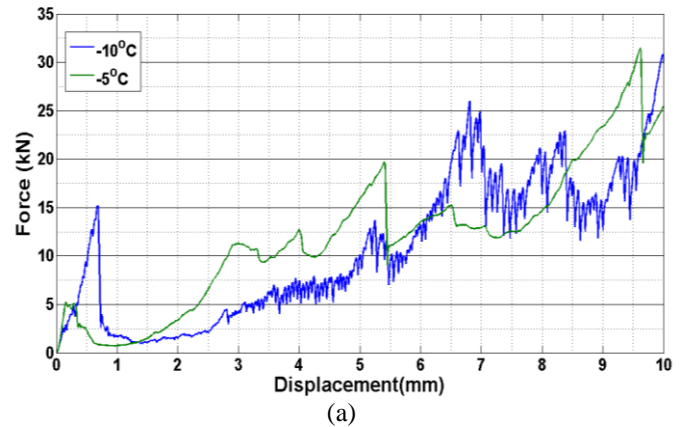

(a)

(b)

Figure 7: (a) MTS load cell data (b) MTS load cell data from 4 to 5 mm displacement for two fast speed tests at different temperatures: Cold test (Test 6: blue) and Warm test (Test 28: green)

The dynamic behaviors based on temperatures can also be observed from the hi-speed video recordings and 'after-crushing' images. In Figure 8 (top) snapshots were taken from the fast speed cold and warm tests just after the indentation had started. The image from the cold test shows that it experienced random failure with spalling and crushing from the very beginning, while the warm test went through comparatively stable and slow crushing failure. This can also be observed in the 'after-crushing' images in Figure 8 (bottom). The warmer sample has a very smooth surface finish after the indentation with a very limited amount of crushed ice in the face of the sample; evidence of a ductile and slow crushing failure. The post-testing image of the cold sample has a rough surface with a large amount of crushed ice on the top, demonstrating that it experienced more dynamic crushing than warmer ice.
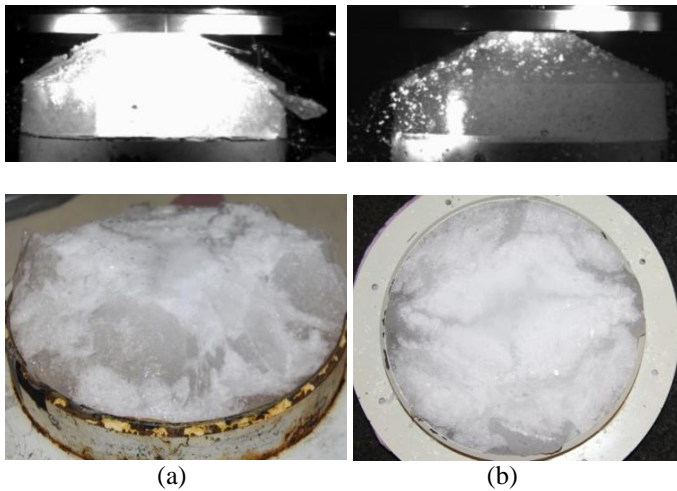

(a)   (b)

Figure 8: Snapshots from hi-speed videos (top) and 'after-crushing' images (bottom) of the samples at two different temperatures (a) -10°C (Test 6) (b) -5°C (Test 28)

Vertical and horizontal thin-section images from medium speed tests in Figure 9 show the effect of temperature on damage. The thin-section pictures that were taken using cross polarized light (color) show that in warmer ice (-5°C) the damaged layer is more heavily dominated by recrystallization as compared to colder (-10°C) ice. From the pictures taken using a side lighting technique (black and white), it is observed that cold tests are dominated by the zones of microfracture. The warm test also showed microfracture in the central zone, but the depth of the damaged layer appears to be larger in the case of the warm ice test than in the cold ice test. This links to the failure processes the samples experienced. As previously mentioned, cold tests, which experience a combination of both fracture and damage failures, typically exhibit more dynamic activity with a large amount of cyclic loading. On the other hand, the warm test showed less dynamics and is characterized by more 'ductile' failure with a deeper, more distributed recrystallized zone.

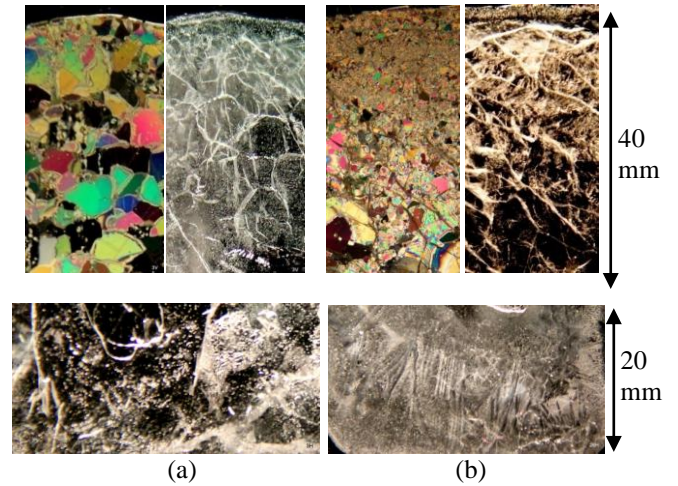(a)   (b)

Figure 9: Vertical (top) and horizontal (bottom) thin-section pictures using cross polarized light (color) and side lighting technique (black and white) (a) Cold test results at -10°C (Test 3) (b) Warm test results at -5°C (Test 26)

Influence of Ice Shape

The shapes of the ice samples were also observed to have a strong influence on failure and crushing behaviors. The images of the three different shaped ice samples having a taper angle of 13°, 21° and 30° that were used in the test program are given in Figure 10. As shown, steeper ice specimens had less volume than flatter ice. Initially, the average mass of the un-crushed specimens were 11.44 kg for 13°, 9.8 kg for 21° and 9.1 kg for 30° ice samples. Given that the flatter ice needed more force to fail than the steeper ice, they have shown some differences in terms of crushing behaviors and dynamic properties.
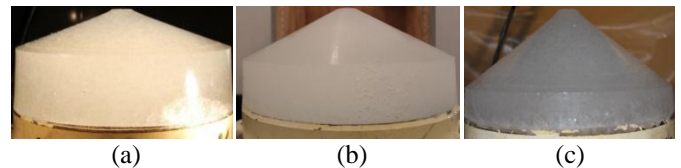

(a)   (b)   (c)

Figure 10: Samples with a taper angle of (a) 13° (b) 21° (c) 30°

The plots of force, area and pressure against time are given in Figure 11 for the three tests having different shaped ice samples. The tests investigated here were done at an indentation rate of 10 mm/s at -10°C and used the spherical indenter. From Figure 11(a) it can be seen that the 13° ice sample showed a higher force than the 21° and 30° ice samples and the amounts of fluctuations in the force appear to be influenced by the shape of the ice samples. These results indicate that the dynamic behavior appears to increase as the ice sample shape become flatter, indicating that the interplay between fracture and damage changes as a function of geometry. In Figure 11(b) the nominal contact area is plotted as a function of time for each of the three taper angles. For the same point in time during a given test (until the indentation reached the cylindrical region of the specimen) the contact area of a 13° taper angle ice sample was larger than for the 21° and 30° ice samples. From the curves of

the nominal pressure against time in Figure 11(c), it can be seen that the mean pressures of ice samples with different taper angles do not vary significantly from the time period between 0.3 and 1 second. The average pressures during this period were close to the same values for all three cases with an average pressure of about 3 MPa.
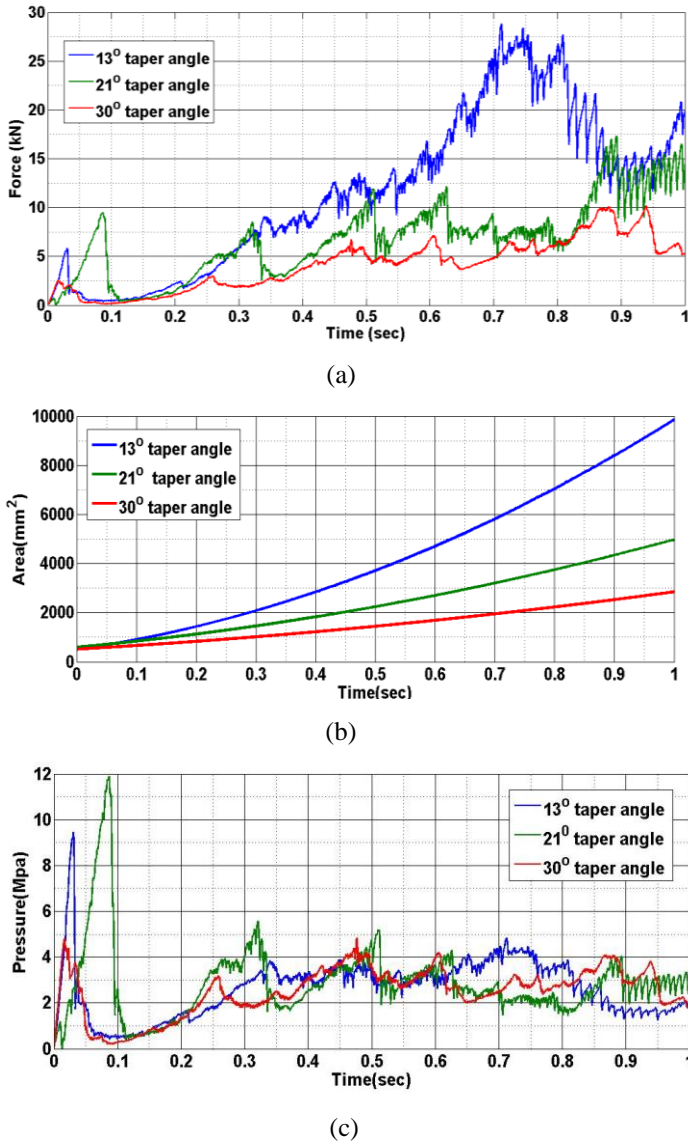

(a)

(b)

(c)

Figure 11: Time traces showing the effects of taper angle for three tests with taper angles of 13° (Test 23), 21° (Test 8) and 30° (Test 9) for: (a) force, (b) area and (c) pressure.

The nature of the dynamics for the ice shapes also show differences in frequencies and amplitudes. For the cyclic loading events considered, the flatter ice specimens experienced lower frequency load cycles but the average amplitudes were higher in these cases. It was also observed that the flatter specimens tended to experience more spalling activity during indentation [33]. When dynamics were observed

from the 13° taper angle ice samples, the dynamic behaviors exhibited a significant interplay between fracture and damage, with the response being lower in frequency and larger in amplitudes. The 30° samples tended to fail in a more continuous crushing mode with less random spalling, as the shape of this specimen promoted the crushing and clearing of ice from under the indenter. The average frequency response, average force amplitude data and average pressure amplitude data for ice samples with different taper angles are shown in Figure 12, Figure 13 and Figure 14, respectively.
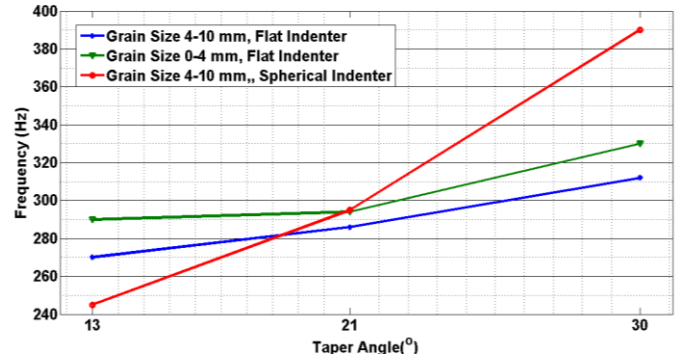

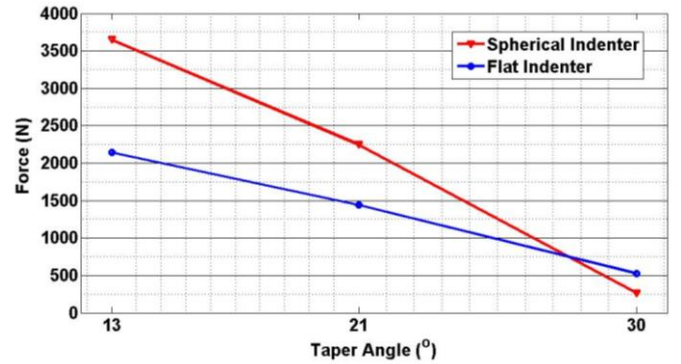Figure 12: Frequency response for different ice shapes

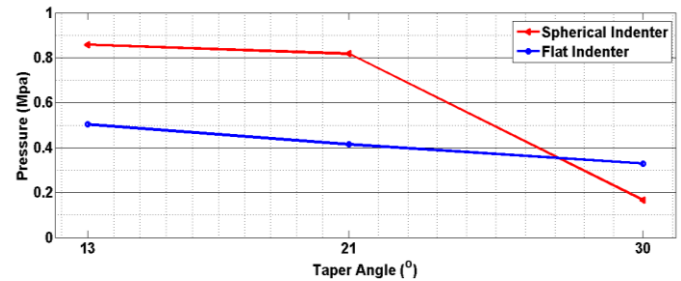Figure 13: Average force amplitudes for different ice shapes

Figure 14: Average pressure amplitudes for different ice shapes

The dynamics and crushing behaviors discussed above can be linked with the thin section pictures given in Figure 15. The tests were done at an indentation rate of 10 mm/s at -10°C using a flat indenter. The images show that the 13° tapered ice

specimen is more dominated by recrystallization as it was exposed to higher localized stresses at an earlier stage of the indentation than were the other cases. These results from the specimen geometry, wherein the indenter reached the cylindrical part of the sample after 25 mm of indentation, whereas for the 21° and 30° ice samples the indenter did not reach the cylindrical part until 46 and 67 mm of indentation, respectively (Figure 10). The 30° tapered ice sample shows less recrystallized microstructure, concentrated in the center indicating that the higher frequency, lower amplitude dynamics are associated with lower amounts of strain than the other cases, which in turn correspond to the observed thinner damaged layers.

40 mm

40 mm

(a) 13°   (b) 21°   (c) 30°
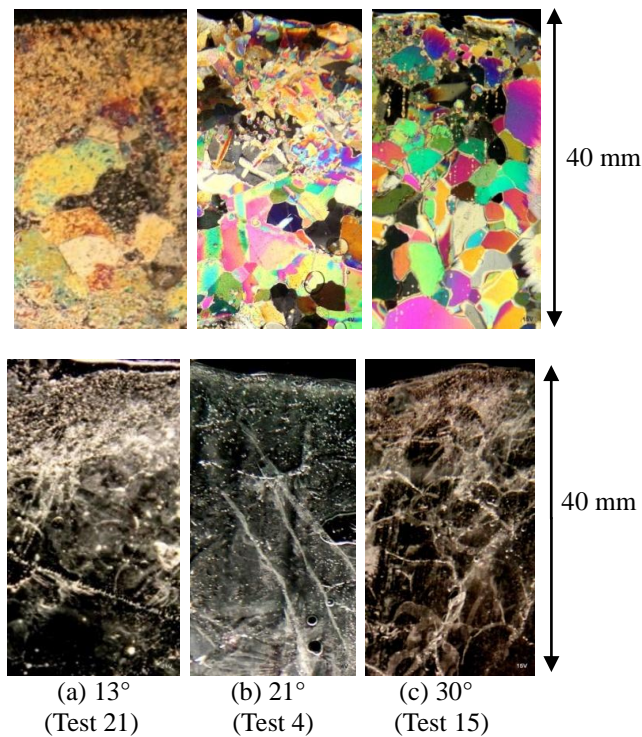(Test 21)   (Test 4)   (Test 15)

Figure 15: Vertical thin-section pictures using cross polarized light (top, color) and side lighting technique (bottom, black and white)

CONCLUSIONS AND FUTURE RECOMMENDATIONS

Small-scale ice indentation tests were conducted to study the nature of compressive ice failure and dynamic crushing behavior. In this study, primary focus was placed on understanding the influence of crushing rate, temperature and ice shape on ice crushing dynamics and failure behavior.

Slow indentation rate tests (0.1 mm/s) were observed to display minimal dynamic behavior. Almost no cyclic loading was noticed throughout the tests, except for the first few seconds when the loads initially began to build up. All of the slow tests, even when different parameters were used, showed similar patterns. Fast speed tests were observed to show more

interplay between spalling and damage failure with a higher amount of dynamic activity. The amplitude of load cycles was observed to be significantly higher than the other cases. Accordingly, it can be concluded for these experiments that if the speeds are higher than 10 mm/s, the dynamic effects are also expected to be higher, but overall total load may be lower. Similarly, in cases of slow speeds (less than 0.1 mm/s), there are no significant dynamics, but they can develop few times more total force than the fast speed tests.

A difference of 5°C in temperature showed a large variation in crushing and dynamic behaviors. The warm ice samples showed a higher force than colder ice throughout the tests, except for some individual crushing and spalling events. However, dynamic effects were more dominant in the cases of the cold tests than the warm tests. Colder tests showed brittle failures with higher cyclic loadings, while the warmer tests showed more ductile failures with minimum dynamic response.

The shapes of the samples showed visible differences in loading patterns, frequencies and amplitudes. The 13° samples required higher forces to fail the specimens and exhibited less frequent amounts of cyclic loading, although when it did occur it tended to have larger average amplitudes when compared to the other cases. Samples with a 30° taper angle showed lower force throughout the test and experienced higher frequencies than flatter ice samples, with a smaller average amplitude of less than 1 kN. It was noticed that the 21° and 13° ice samples have 4 and 7 times higher force amplitudes, respectively, than 30° ice samples.

In summary, ice dynamics and crushing behaviors were observed to depend largely on the loading rate, temperature and geometry of the ice samples. The tests conducted for this research were unconfined and small-scale. To understand the practical situation it is also important to include the effect of confinement in the analysis of ice crushing dynamics using medium and large-scale tests. For this reason, plans are underway for a new series of medium-scale experiments to study the indentation of confined ice specimens over a similar range of nominal interaction areas using spherical indenters.

REFERENCES

[1] Peyton, H. R., 1968. Ice and Marine Structure, Part II: Sea Ice Properties. Ocean Indus., 3, pp. 59–65.

[2] Blenkarn, K.A., 1970. Measurement and analysis of ice forces on Cook Inlet structures. Proceedings, Offshore Technology Conference, Houston, paper OTC1261, vol. 2, pp. 365–378.

[3] Neill, C., 1976. Dynamic Ice Forces on Piers and Piles: An Assessment of Design Guidelines in the Light of Recent Research. Can. J. Civ. Eng., 3, pp.305–341

[4] Engelbrektson, A., 1977. Dynamic ice loads on lighthouse structures. In Proc. 4th Int. Conf. on Port and Ocean Engrg. under Arctic Conditions, St. John's, Canada.

[5] Määttänen, M., 1988. Ice-Induced Vibrations of Structures–Self-Excitation. In Proceedings of the IAHR International Symposium on Ice, Sapporo, pp. 658-664.

[6] Sodhi, Devinder S., 1988. Ice-Induced Vibrations of Structures. In Proceedings of IAHR Ice Symposium on Ice, Sapporo, pp. 625-657.

[7] Jordaan, I. J. and Timco, G. W. ,1988. Dynamics of the Ice-Crushing Process. Journal of Glaciology, Vol. 34, No. 118, pp 318-326.

[8] Karna, T. and Turunen, R., 1989. Dynamic Response of Narrow Structures to Ice Crushing. Cold Regions Science and Technology, Vol. 17. Elsevier Science Publishers B.V., Amsterdam, pp.173-187.

[9] Karna, T. and Turnunen, R., 1990. A straightforward technique for analyzing structural response to dynamic ice action. In Proc. of 9th Int. Offshore Mech. And Arctic Eng., Vol. IV, Houston, pp. 135–142.

[10] Yue, Q.J. and Bi, X.J., 1998. Full-scale tests and analysis of dynamic interaction between ice sheet and conical structures. In Proc. of 14th International Association for Hydraulic Research (IAHR), Vol. II, Symposium on Ice, Potsdam.

[11] Yue Q.J. and Bi X.J., 2000. Ice-induced Jacket Structure Vibrations Bohai Sea. Journal of Cold Regions Engineering [ASCE] 14(2), pp. 81-92.

[12] Jordaan, I.J., 2001. Mechanics of ice-structure interaction. Engineering Fracture Mechanics; 68, pp.1923-1960.

[13] Sodhi, D.S., 2001. Crushing failure during ice-structure interaction. Engineering Fracture Mechanics, 68, pp. 1889–1921.

[14] Huang, G., Liu, P.,2009. Journal of Offshore Mechanics and Arctic Engineering, 2009. Vol. 131/011501-1.

[15] Palmer, A., Yue, Q., Guo, F., 2010. Ice Induced vibration and scaling. Cold Regions Science and Technology. vol. 60 (2010), pp. 189-192.

[16] Xu, N.; Yue, Q., 2014. Journal of Offshore Mechanics and Arctic Engineering, 2014. Vol. 136/014501-1.

[17] Matlock, G., Dawkins, W., and Panak, J., 1971. Analytical Model for Ice-Structure Interaction. J. Eng. Mech. Div., EM4, pp. 1083–1092.

[18] Sodhi, D. S., 1995. An Ice-Structure Interaction Model. Mechanics of Geomaterial Interfaces, APS Selvadurai and MJ Boulon, Eds, Amsterdam, Elsevier, pp 57–75.

[19] Määttänen, M., 1978. On conditions for the rise of self-excited ice-induced autonomous oscillations in slender marine pile structures. Styrelsen för vintersjöfartsforskning (Winter Navigation Research Board, Finland), research report, vol. 25.

[20] ISO 19906 Standard, 2009. Petroleum and Natural Gas Industries-Arctic Offshore Structures.

[21] Yue, Q., Guo, F., Kärnä, T., 2009. Dynamic ice force of slender vertical structures due to ice crushing. Cold Regions Science and Technology. vol. 56 (2−3), pp. 77–83.

[22] Bjerkås, M., 2006. Ice actions on offshore structures. PhD thesis. Norwegian University of Science and Technology.

[23] Bjerkås, M., Skiple, A., 2005. Occurrence of continuous and intermediate crushing during ice-structure interaction. Proceedings, Eighteenth International Conference on Port and Ocean Engineering under Arctic Conditions, St. John's.

[24] Jefferies, M.G., Wright, W.H., 1988. Dynamic response of Molikpaq to ice-structure interaction. Proceedings, Seventh International Conference on Offshore Mechanics and Arctic Engineering Symposium, Houston, pp. 201–220.

[25] Taylor, R.S., 2010. Analysis of Scale Effect in Compressive Ice Failure and Implications for Design. Ph.D Thesis, Memorial University, St. John's, NL, Canada.

[26] Wells, J., Jordaan, I., Derradji-Aouat, A. and Taylor, R., 2010. Small-scale laboratory experiments on the indentation failure of polycrystalline ice in compression: Main results and

pressure distribution. Cold Regions Science and Technology, Vol. 65, No. 3, pp. 314-325.

[27] Browne, T., 2012. Analysis of Compressive Ice Failure during Ice-structure Interaction. M. Eng Thesis. Memorial University of Newfoundland. St. John's, Canada .

[28] Browne, T., Taylor, R.S., Jordaan, I., Gürtner, A., 2013. Small-scale Ice Indentation Tests with Variable Structural Compliance. Cold Regions Science and Technology, Volume 88, April 2013, pp. 2-9.

[29] Taylor, R.S., Browne, T., Jordaan, I., Gürtner, A., 2013. Fracture and Damage during Dynamic Interactions between Ice and Compliant Structures at Laboratory Scale. Proceedings of Offshore Mechanics and Arctic Engineering Conference, Nantes, France.

[30] Taylor, R.S., Jordaan, I.J., 2015. Probabilistic fracture mechanics analysis of spalling during edge indentation in ice. Engineering Fracture Mechanics. 134 (2015) 242-266.

[31] Jordaan, I. J., Wells, J., Xiao, J., Derradji-Aouat, A., 2008. Ice crushing and cyclic loading in compression. Proceedings 19th IAHR Symposium on Ice, Vancouver, British Columbia, Canada.

[32] Taylor, R.S., Frederking, R, and Jordaan, I. J. (2008). The nature of high pressure zones in compressive ice failure. Proceedings 19th IAHR Symposium on Ice,Vancouver, British Columbia, Canada .

[33] Habib, K. B., 2014. Experimental Investigation of compressive failure of truncated conical ice specimen. Master's Thesis, Memorial University of Newfoundland, St. John's, Newfoundland, Canada.

[34] Habib, K. B. ,Taylor, R.S., Jordaan, I., Bruneau, S., 2014. Experimental Investigation Of Compressive Failure Of Truncated Conical Ice Specimens. Proceedings of Offshore Mechanics and Arctic Engineering Conference, San Fransisco, USA.

[35] Barrette, P., Pond, J., and Jordaan, I., 2002. Ice damage and layer formation in small scale indentation experiments. Ice in the Environment, Proceedings of the 16th international Symposium on Ice, IAHR, Dunedin, New Zealand, vol. 3, pp. 246-253.

[36] Dillenburg, A. K., 2012. Rate dependency in conical ice indenter failure. Master's Thesis, University of Duisburg-Essen, Institute of Ship Technology, Ocean Engineering and Transport Systems.

[37] Bruneau, S., Dillenburg, A., Ritter, S., 2011. Ice Specimen Fabrication Techniques and Indentation Experiments, A StePS[2] Pilot Laboratory Investigation of Ice-Structure Interaction" STEPS-RP001-2011. Memorial University of Newfoundland, Sustainable Technology for Polar Ships and Structures, St. John's, NL, Canada , P. 139.

[38] Bruneau, S., Dillenburg, A., Ritter, S., 2012. Ice Sample Production Techniques and Indentation Tests for Laboratory Experiments Simulating Ship Collisions with Ice. Rhodos, Greece.

[39] Bruneau, S., Colbourne, B., Dragt, R., Dillenburg, A., Ritter, S., Pilling, M., Sullivan, A., 2013. Laboratory Indentation Tests Simulating Ice-Structure Interactions Using Cone-Shaped Ice Samples and Steel Plates. POAC. Espoo, Finland.

[40] Dragt, R.C., Bruneau, S.E., 2013. The Collision of Cone Shape Ice Samples against Steel Plates of Varying Surface Roughness. POAC. Espoo, Finland.

[41] Jones. S. J.,Gagnon, R.E., Derradji, A.,and Bugden,A., 2003. Compressive strength of iceberg ice. Canadian Journal of Physics.

[42] Sinha, N.K., 1977. Technique for studying the structure of sea ice. Journal of Glaciology, Vol-18, pp. 315-323.